Neurocomputing 129 (2014) 94–106

Contents lists available at ScienceDirect

Neurocomputing

journal homepage: www.elsevier.com/locate/neucom

Emotional state classification from EEG data using machine learning approach

Xiao-Wei Wang [a], Dan Nie [a], Bao-Liang Lu [a,b,*]

[a] Center for Brain-Like Computing and Machine Intelligence, Department of Computer Science and Engineering, Shanghai Jiao Tong University, 800 Dong Chuan Road, Shanghai 200240, China

[b] MOE-Microsoft Key Laboratory for Intelligent Computing and Intelligent Systems, Shanghai Jiao Tong University, 800 Dong Chuan Road, Shanghai 200240, China

ARTICLE INFO

Article history:
Received 17 February 2012
Received in revised form
6 June 2013
Accepted 14 June 2013
Available online 8 November 2013

Keywords:
Emotion classification
Electroencephalograph
Brain–computer interface
Feature reduction
Support vector machine
Manifold learning

ABSTRACT

Recently, emotion classification from EEG data has attracted much attention with the rapid development of dry electrode techniques, machine learning algorithms, and various real-world applications of brain–computer interface for normal people. Until now, however, researchers had little understanding of the details of relationship between different emotional states and various EEG features. To improve the accuracy of EEG-based emotion classification and visualize the changes of emotional states with time, this paper systematically compares three kinds of existing EEG features for emotion classification, introduces an efficient feature smoothing method for removing the noise unrelated to emotion task, and proposes a simple approach to tracking the trajectory of emotion changes with manifold learning. To examine the effectiveness of these methods introduced in this paper, we design a movie induction experiment that spontaneously leads subjects to real emotional states and collect an EEG data set of six subjects. From experimental results on our EEG data set, we found that (a) power spectrum feature is superior to other two kinds of features; (b) a linear dynamic system based feature smoothing method can significantly improve emotion classification accuracy; and (c) the trajectory of emotion changes can be visualized by reducing subject-independent features with manifold learning.

1. Introduction

Emotion plays an important role in human–human communication and interaction. The ability to recognize the emotional states of people surrounding us is an important part of natural communication. Considering the explosion of machines in our commonness, emotion interaction between humans and machines has been one of the most important issues in advanced human–machine interaction and brain–computer interface today [1]. To approach the affective human–machine interaction, one of the most important prerequisites is to develop a reliable emotion recognition system, which can guarantee acceptable recognition accuracy, robustness against any artifacts, and adaptability to practical applications.

Numerous studies on engineering approaches to automatic emotion recognition have been performed in the past few decades. They can be categorized into three main approaches. The first kind of approaches focuses on the analysis of facial expressions or speech [2–4]. These audio-visual based techniques allow noncontact detection of emotion, so they do not give the subject any discomfort. However, these techniques might be more prone to deception, and the parameters easily vary in different situations. The second kind of approaches focuses on periphery physiological signals. Various studies show that peripheral physiological signals changing in different emotional states can be observed on changes of autonomic nervous system in the periphery, such as electrocardiogram (ECG), skin conductance (SC), respiration, and pulse [5–7]. In comparison with audio-visual based methods, the responses of peripheral physiological signals tend to provide more detailed and complex information as an indicator for estimating emotional states.

The third kind of approaches focuses on brain signals captured from central nervous system such as electroencephalograph (EEG), electrocorticography (ECoG), and functional magnetic resonance imaging (fMRI). Among these brain signals, EEG signals have been proven to provide informative characteristics in responses to the emotional states [8–10]. Since Davidson et al. [11] suggested that frontal brain electrical activity was associated with the experience of positive and negative emotions, the studies of associations between EEG asymmetry and emotions have been received much

* Corresponding author at: Center for Brain-Like Computing and Machine Intelligence, Department of Computer Science and Engineering, Shanghai Jiao Tong University, 800 Dong Chuan Road, Shanghai 200240, China.
Tel.: +86 21 3420 5422; fax: +86 21 3420 4728.
E-mail addresses: bllu@sjtu.edu.cn, blu@cs.sjtu.edu.cn (B.-L. Lu).

0925-2312/$ - see front matter © 2013 Elsevier B.V. All rights reserved.
http://dx.doi.org/10.1016/j.neucom.2013.06.046

attention [12–14]. Besides the EEG asymmetry for the study of emotion, event-related potentials indexing a relatively small proportion of mean EEG activity were also been used to study the association with EEG and emotion [15–17]. However, these approaches still suffer from two problems. The first one is that the existing approaches need to make an average of EEG features. This makes them need longer time windows to recognize the emotion state based on EEG signals. The other one is that only the relatively small percentage of EEG activity that can be captured. These limitations make the existing methods inappropriate or insufficient for assessing emotion states for real-world applications.

With the rapid development of dry electrode, digital signal processing, machine learning, and various real-world applications of brain–computer interface for normal people, more and more researchers focused on EEG-based emotion recognition in recent years, and various approaches have been developed. However, there still exist some limitations on traditional EEG-based emotion recognition framework. One of the major limitations is that almost all existing approaches do not consider the characteristics of EEG and emotion. As EEG is an unsteady voltage signal, the feature extracted from EEG usually changes dramatically, whereas emotion states change gradually. This leads to bigger differences among EEG features, even with the same emotion state in adjacent time. Moreover, existing studies can only predict the labels of emotion samples, but could not reflect the trend of emotion changes. To overcome these shortcomings, in this paper, we introduce a feature smoothing method and an approach to tracking the trajectory of emotion changes. To validate the effectiveness of the proposed methods, we compare three kinds of EEG emotion-specific features, and evaluate the performance of classification of two emotion states from EEG data of six subjects.

The rest of this paper is structured as follows. In Section 2, we give a brief overview of related work on emotion models, effect of movie in emotion induction, and various methods for EEG-based emotion classification. Section 3 gives the motivation and rationale for our experimental setting of emotion induction. A systematic description of feature extraction, feature smoothing, feature dimensionality reduction, classification, and trajectory of emotion changes is given in Section 4. In Section 5, we present experimental results that we achieved, and conclusions and feature work are presented at the end.

2. Related work

2.1. Models of emotions

As all people express their emotions differently, it is not an easy task to judge and model human emotions. Researchers often use two different methods to model emotions. One approach is to organize emotion as a set of diverse discrete emotions. In this model, there is a set of emotions which are more basic than others, and these basic emotions can be seen as prototypes from which other emotions are derived. The problem with this method is that there is still little agreement among scientists about how many and which emotions are basic until now. Different theorists consider different emotions to be basic. For example, Weiner thought only happiness and sadness to be basic [18], whereas Kemper suggested fear, anger, depression and satisfaction to be basic [19]. Another way is to use multiple dimensions or scales to categorize emotions. The two dimensional model of emotion is described by Davidson et al. [20]. According to this model, emotions are specified by their position in the two-dimensional space as shown in Fig. 1, which is spanned by two axes of valence in horizontal axis and arousal in vertical axis. Valence represents the quality of an emotion ranging from unpleasant to pleasant.

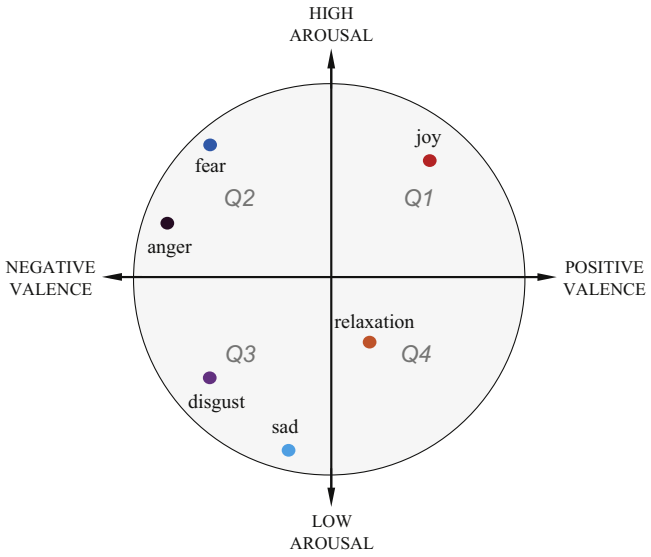

Fig. 1. Two-dimensional emotion model.

Arousal refers to the quantitative activation level ranging from calm to excited. The different emotional labels can be plotted at various positions on a 2D plane spanned by these two axes. In addition to the 2D model, some researchers have subsumed these associated action tendencies in a 3D emotion model, which includes arousal, valence, and dominance. Here, dominance refers to the degree to which the person feels unrestricted or in control of a situation ranging from weak to strong [21].

2.2. Movie and emotion

Many different materials have been used to elicit emotions in the laboratory such as facial expressions [22], slides [23], texts [24], music [25], and movies [26]. Among these materials, movies have the desirable properties of being readily standardized, involving no deception and being dynamic rather than static. The properties of dynamic visual and audio stimuli make movies seem to be one of the most effective ways to elicit emotions.

The development of using movies as emotions elicitors has paralleled with wider maturation of emotion science. For much of the past half-century, movies have been selected to elicit a diffuse state of anxiety or stress [27]. Recently, there has been increasing interest in studying more differentiated emotional states. Researchers working within dimensional studies tried to elicit specific emotional states, such as valence and intensity [28], while researchers advocating a discrete emotion model tried to elicit specific target emotions. Philippot [29] reported on a movie set, which included two clips for each of the target emotional states such as happiness, fear, disgust, anger, sadness, and neutral. Hewig et al. [30] developed a set of 20 movie clips that could be used to induce six emotional states, namely angry, disgust, fear, sadness, amusement and neutral. Gross et al. [31] found a set of 16 movie clips that reliably elicit each of eight emotions, namely amusement, anger, contentment, disgust, fear, neutral, sadness, and surprise.

2.3. EEG and emotion

Since brain emotional system is a substrate for emotion related processes, EEG can reveal important information on their functioning. The studies of associations between EEG activity and emotions have been received much attention [32–34]. A number of these studies have focused on the question of asymmetrical

activation of the cerebral hemisphere. Davidson et al. [35] detected that greater relative left frontal EEG activity is related to positive related emotion, while greater relative right frontal EEG activity is related to negative, withdrawal-related emotion. Likewise, in an EEG study about brain asymmetries during reward and punishment, Henriques et al. [36] found a pattern of greater relative right frontal EEG activity in depressed adults. In an experiment where emotions were induced with visual and auditory stimuli, Baumgartner et al. [37] showed that EEG activity over the left hemisphere increases in happy conditions compared to negative emotional conditions. Besides the research of asymmetrical activation of the cerebral hemisphere, event-related potentials were also been used to study the association with EEG and emotion. Vanderploeg et al. [38] reported that the presentations of the photos with emotional facial expressions elicited more negative amplitudes during 230 $\pm$420 ms (with peak at about 340 ms) after the stimulus onset than did neutrally rated stimuli. Wataru et al. [39] reported that the visual presentations of the faces with emotion (both fear and happiness) elicited a larger N270 over the posterior temporal areas, covering a broad range of posterior visual areas. Carretie et al. [40] found that P200, an attention-related component, showed higher amplitudes and shorter latencies in response to negative stimuli than in response to positive stimuli.

Since EEG not only indicates emotional states, but also reflects other cognitive activity of the brain. The choice of independent variables to discriminate emotions from the range of EEG and electrode locations is not very self-evident, thus recently researchers tried to use more complex methods to find the correlation between the emotional changes and EEG signals. Chanel et al. [41] proposed an emotion recognition system that uses EEG to classify two emotional states. Their research achieved a classification accuracy of 72% for naive Bayes and 70% for Fisher discriminant analysis. Li et al. [42] used EEG signals to recognize emotion in response to emotional pictures. Their study achieved a recognition rate of 93.5% for two emotional states. Zhang et al. [43] reported an average accuracy of 73.0% by using EEG features to categorize subject's status into two emotional states. Murugappan et al. [44] showed an emotion recognition approach using different set of EEG channels with a maximum accuracy of 83.26% for five emotional states. Petrantonakis et al. [45] demonstrated a user-independent emotion recognition system. For six emotion categories, a recognition rate of 83.33% was achieved.

3. Materials

3.1. Stimulus material and presentation

To stimulate subject's emotions, we used a set of movie clips that was mainly extracted from Oscar films as elicitors. As shown in Table 1, the movie clips set includes six clips for each of two target emotional states: positive and negative emotions. The selection criteria for movie clips were as follows: (a) the length of the scene should be relatively short; (b) the scene is to be understood without explanation; and (c) the scene should elicit single desired target emotion of subjects. To evaluate whether the movie clips excite specified emotional states or not, we carried out an investigation using questionnaires from twenty-six subjects who did not take part in the experiment to verify the effectiveness of these elicitors before the experiment.

3.2. Participants

Six right-handed health volunteers (three males and three females), 18–25 years of age (mean = 22.1 and SD = 1.25), participated in the study. All subjects had no personal history of neurological or

Table 1
Description of the movie clips.

Number	Film title	Target emotion	Company	Year
1	King Kong	Negative	Big Primate Pictures, etc.	2005
2	Titanic	Negative	Twentieth Century Fox, etc.	1997
3	Schindler's List	Negative	Universal Pictures, etc.	1993
4	Silent Hill	Negative	Silent Hill DCP Inc., etc.	2006
5	The Day After Tomorrow	Negative	Centropolis Entertainment, etc.	2004
6	The Silence of the Lambs	Negative	Orion Pictures Corporation, etc.	1991
7	The Sound of Music	Positive	Robert Wise Productions, etc.	1965
8	High School Musical	Positive	First Street Films, etc.	2006
9	Sister Act	Positive	Touchstone Pictures	1992
10	Nature Time Lapse I	Positive	Mockmoon	2009
11	Nature Time Lapse II	Positive	Mockmoon	2009
12	Nature Time Lapse III	Positive	Mockmoon	2009

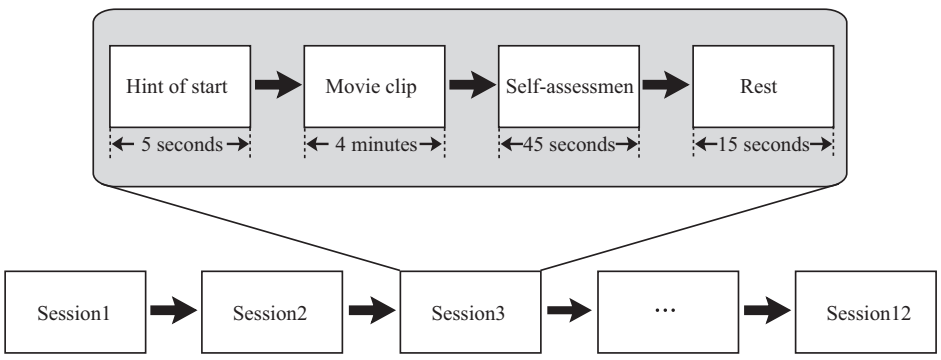

Fig. 2. The process of experiment.

psychiatric illness and had normal or corrected-normal vision. All of the subjects were informed the scope and design of the study.

3.3. Task

In order to get quality data, the subjects were instructed to keep their eyes open and view each movie clip for its entire duration in the experiment. The process of our experiment is depicted in Fig. 2. Movie clips inducing different emotional states were presented in a random order. Each movie clip was presented for 3–5 min, preceded by 5 s of blank screen as the hint of start. At the end of each clip, the subjects were asked to assign valence, arousal and dominance ratings and rate the specific emotions they had experienced during movie viewing. The rating procedure lasted about 45 s. An inter-trial interval (15 s) of blank screen lapsed between movie presentations for emotion recovery.

Valence, arousal and dominance ratings were obtained using the self-assessment manikin (SAM) shown in Fig. 3 [46]. The given self-reported emotional states were used to verify EEG-based emotion classification. In this paper, we only chose the sessions whose dominance ratings were equal to or larger than 3. The reason was that if the dominance rating was smaller than 3, we assumed that this session did not successfully arouse a certain emotion of the subject. Furthermore, we only cared about two kinds of emotional states, namely positive and negative emotions. If the valence rating was smaller than 5, then this session belonged to the class of negative emotion, else it belonged to the class of positive emotion.

3.4. EEG recording

A 128-channel electrical signal imaging system (ESI-128, NeuroScan Labs), SCAN 4.2 software, and a modified 64-channel QuickCap with embedded Ag/AgCl electrodes were used to record EEG data. Each subject was fitted with a 62-channel electrode cap, whose electrodes were arranged according to the extended international 10–20 system. The ground electrode was attached to the center of the forehead, and the reference electrode was located at the vertex of the head. The impedance was kept below 5 k Ω. The EEG data were recorded with 16-bit quantization level at the sampling rate of 1000 Hz. Electrooculogram (EOG) was also recorded, and later used to identify blink artifacts from the recorded EEG data.

4. Methods

The EEG data we got from the experiments were analyzed through several procedures, including signal preprocessing, feature extraction, feature smoothing, feature dimensionality reduction, emotional state classification and trajectory of emotion changes, as shown in Fig. 4.

4.1. Signal preprocessing

First, the EEG signals were down-sampled to a sampling rate of 200 Hz to reduce the burden of computation. Second, the time waves of the EEG data were visually checked. The recordings seriously contaminated by electromyogram (EMG) and electrooculogram were removed manually. Third, each channel of the EEG data was divided into same-length epochs without overlapping using time-windows. Finally, all features discussed below were computed on each epoch of the EEG data.

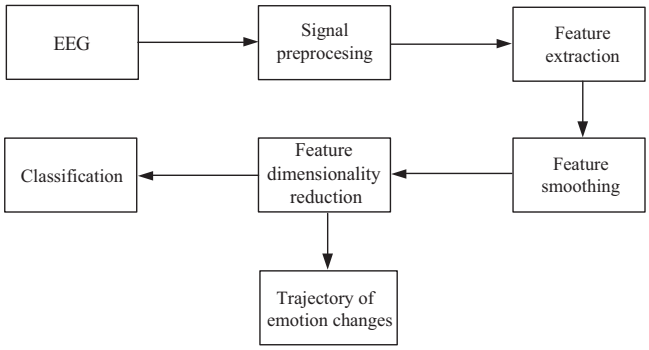

Fig. 4. The flowchart of emotional state classification from EEG data.

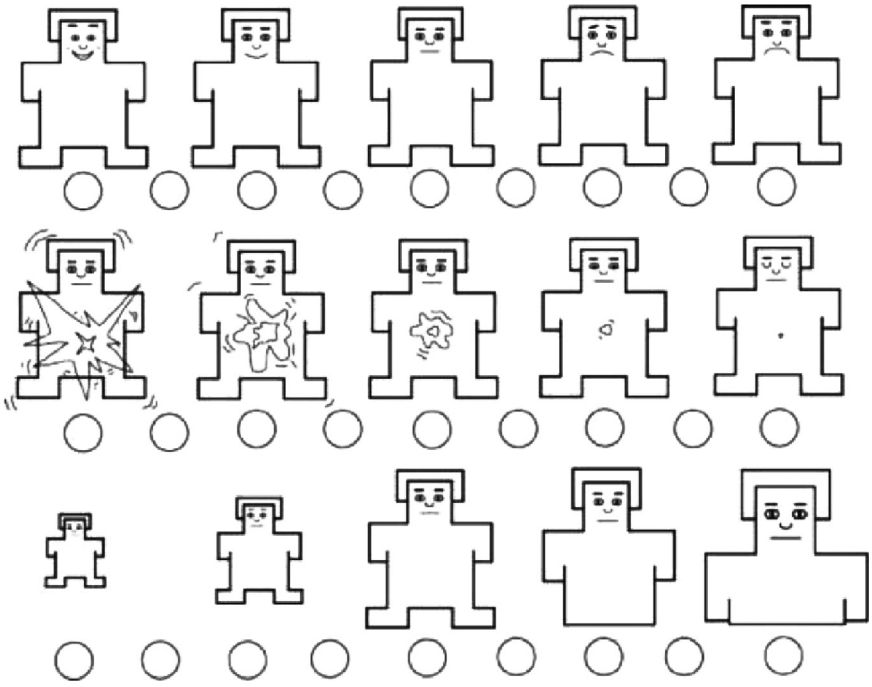

Fig. 3. The self-assessment manikin.

4.2. Feature extraction

The main task of feature extraction is to derive the salient features which can map the EEG data into consequent emotional states. For a comparison study, we investigated three kinds of emotion-specific features, namely power spectrum, wavelet and nonlinear dynamical analysis.

4.2.1. Power spectrum feature

Power spectrum can be analyzed to characterize the perturbations in the oscillatory dynamics of ongoing EEG [47,48]. First, each epoch of the EEG data was processed with Hanning window. Second, windowed epochs were extended by zero padding for a fast Fourier transform (FFT). Finally, EEG power spectrums were log-transformed after being extracted in different bands such as delta rhythm (0.5–4 Hz), theta rhythm (4-8 Hz), alpha rhythm (8–13 Hz), beta rhythm (13–30 Hz) and gamma rhythm (30–50 Hz). Besides power spectrum of all electrodes, the power spectrum of differential asymmetry was also chosen as EEG power spectrum features. Throughout the whole brain, there were 27 asymmetry indices derived from 27 symmetric electrode pairs, namely FP1–FP2, AF3–AF4, F1–F2, F3–F4, F5–F6, F7–F8, FC1–FC2, FC3–FC4, FC5–FC6, FT7–FT8, C1–C2, C3–C4, C5–C6, T7–T8, CP1–CP2, CP3–CP4, CP5–CP6, TP7–TP8, P1–P2, P3–P4, P5–P6, P7–P8, PO3–PO4, PO5–PO6, PO7–PO8, CB1–CB2, O1–O2. The power spectrum of differential asymmetry was calculated by power spectrum subtraction (e.g. power spectrum of C3 minus power spectrum of C4).

4.2.2. Wavelet feature

Wavelet feature is the typical time–frequency domain feature that was used for EEG signal analysis [49]. In this study, the Daubechies wavelet of order four was used to analyze the EEG data. This wavelet function was chosen due to its near optimal time–frequency location properties [50]. The wavelet transform performs a time–frequency decomposition of the signal, *i.e.* at each resolution level and each time position. The wavelet function is correlated with the shape of the waveform at that position. This correlation, known as a wavelet coefficient, measures how much of the wavelet at that resolution level and position is included in the EEG waveform.

Table 2 presents that after a five octave wavelet decomposition, the coefficients were obtained with a sampling frequency of 200 Hz. It can be seen that the components of these decompositions: A5 decomposition is nearly within the delta range (0.5–4 Hz), D5 decomposition is nearly within the theta range (4–8 Hz), D4 decomposition is nearly within the alpha range (8–13 Hz), D3 decomposition is nearly within the beta range (13–30 Hz), and D2 decomposition is nearly within the gamma range (30–50 Hz).

Since the coefficients from each resolution level j correspond to different frequency bands, the energy E_j for each frequency range in each time window can be computed as the corresponding squared coefficients. Total energy E_{total} of the signal in each time window was calculated as the sum of energies of all resolution levels. Thereafter, the relative wavelet energy $P_j = E_j/E_{total}$ was computed as the ratio between the energy of each level. Then, the wavelet entropy W_e can be defined as

$$W_e = \sum_{i=1}^{n} P_j \ln P_j \tag{1}$$

The wavelet coefficient energy E_j and the wavelet entropy W_e were chosen as the time–frequency domain features in this study.

Table 2
Frequencies corresponding to different levels of decomposition for Daubechies wavelet of order four with a sampling frequency of 200 Hz.

Decomposed signal	Frequency range (Hz)
D1	50–100
D2	25–50
D3	12.5–25
D4	6.25–12.5
D5	3.125–6.25
A5	0–3.125

4.2.3. Nonlinear dynamical feature

The importance of the biological time-series analysis, which exhibits typically complex dynamics, has been recognized in the area of non-linear analysis [51]. Several features of these approaches have been proposed to detect the hidden important dynamical properties of the physiological phenomenon. In this paper, we studied the EEG signals using three different kinds of nonlinear dynamical features, namely approximate entropy, hurst exponent and fractal dimension.

Approximate entropy is a family of statistics and is claimed to be a non-linear quantification of the regularity of a signal [52,53]. Approximate entropy takes into account the temporal order of points in a time sequence and is therefore a preferred measure of randomness or regularity. The first step in computing approximate entropy of a time series x_i, $i = 1, \ldots, n$, is to construct the state vectors in the embedding space:

$$y_i = \{x_i, x_{i+1}, x_{i+2}, \ldots, x_{(i+m-1)}\}, 1 \le i \le n-m+1 \tag{2}$$

where m is the embedding dimension. Second, we define

$$C_i^m(r) = \frac{1}{n-m+1} \sum_{j=1}^{n-m+1} \theta(r - d(y_i, y_j)) \tag{3}$$

where $\theta(y)$ ($\theta(y) = 1$ for $y > 0$, $\theta(y) = 0$, otherwise) is the standard heavyside function, r is the vector comparison distance, and $d(y_i, y_j)$ is a distance measure defined by

$$d(y_i, y_j) = \max_{k=1,2,\ldots,m} (|y_{(i+k-1)} - y_{(j+k-1)}|) \tag{4}$$

Third, we define $\phi^m(r)$ as

$$\phi^m(r) = \frac{1}{n-m+1} \sum_{i=1}^{n-m+1} \ln C_i^m(r) \tag{5}$$

Finally, for fixed m, r, and n, approximate entropy A_e can be expressed as

$$A_e(m, r, n) = \phi^m(r) - \phi^{m+1}(r) \tag{6}$$

Hurst exponent is the measure of the smoothness of a fractal time series based on the asymptotic behavior of the rescaled range of process [54]. In time series analysis, hurst exponent is used by Kannathal et al. for characterizing the nonstationary behavior of the EEG episodes [55,56]. Assuming a time series $x_i, i = 1, \ldots, n$, the mean value is defined as

$$m = \frac{1}{n} \sum_{i=1}^{n} x_i \tag{7}$$

The deviation from the mean m for the first k data points is defined as

$$W_t = \sum_{j=1}^{t} x_j - tm, \quad t = 1, 2, \ldots, n \tag{8}$$

and then the difference between the maximum value and minimum value of the deviation corresponding to n is acquired by

$$R(n) = \max(0, W_1, \ldots, W_n) - \min(0, W_1, \ldots, W_n) \tag{9}$$

If $S(n)$ denotes the standard deviation of the time series $x_i, i = 1, \ldots, n$, the rescaled range $R(n)/S(n)$ is the average over all the partial time series of length n. The hurst exponent H can be

estimated by fitting to the data using the power law:

$$\mathrm{E}\left[\frac{R(n)}{S(n)}\right] = Cn^H \tag{10}$$

where $\mathrm{E}[R(n)/S(n)]$ is the expected value of $R(n)/S(n)$.

The term 'fractal' was first introduced by Mandelbrot [57]. The concept of fractal dimension that refers to a non-integer or fractional dimension originates from fractal geometry. This feature has been used in the analysis of EEG to identify and distinguish specific states of physiological function. Many algorithms are available to determine the fractal dimension of the waveform. In this work, we used the Katz algorithm [58]. We chose to use this method because it was widespread in EEG literature [59]. The fractal dimension F_d of a planar is defined as follows:

$$F_d = \frac{\ln(n)}{\ln(d)} \tag{11}$$

where n is the total length of the EEG time series and d is the Euclidean distance between the first point in the series and the point that provides the furthest distance with respect to the first point. The fractal dimension compares the actual number of units required to reproduce a pattern of the same spatial extent. Fractal dimension computed in this faction depends upon the measurement units used. To resolve this problem, Katz proposed a normalization as follows:

$$F_d = \frac{\ln(n/\underline{a})}{\ln(d/\underline{a})} = \frac{\ln(k)}{\ln(k)+\ln(d/n)} \tag{12}$$

where $\underline{a}$ is the average number of steps in the series and k is n divided by $\underline{a}$.

4.3. Feature smoothing

Although emotional states usually change gradually, features extracted directly from EEG data always have strong fluctuations and contain some information unrelated to the emotion task. Therefore, we should smooth the features to minimize the presence of artifacts in the EEG features. As emotional states are time-dependent, the features extracted from EEG components are also time-dependent. Thus, we could represent a state space model in the form of linear dynamical system (LDS) to filter out the above influences [60].

Let $\mathbf{y}_t$, $t=1,\ldots,n$, refer to the observation feature sequence, each of which is m dimension, $\mathbf{y}_t=(y_{t1},y_{t2},\ldots,y_{tm})^T$ (usually $m<n$), and $\mathbf{x}_t$ represent the latent state feature sequence. The LDS approach is described by

$$\mathbf{x}_{t+1} = \mathbf{A}\mathbf{x}_t + \mathbf{w}_t, \quad \mathbf{w}_t \sim \mathcal{N}(0,\boldsymbol{\Gamma}) \tag{13}$$

$$\mathbf{y}_{t+1} = \mathbf{C}\mathbf{x}_t + \mathbf{e}_t, \quad \mathbf{e}_t \sim \mathcal{N}(0,\boldsymbol{\Sigma}) \tag{14}$$

where $\mathbf{A}\in\mathbb{R}^{m\times m}$ is the transition probability matrix and $\mathbf{C}\in\mathbb{R}^{m\times m}$ is the emission probability matrix. The output $\mathbf{y}_t$ is a linear function of the state $\mathbf{x}_t$ which evolves through first-order Markov chain. Both state and output noise, $\mathbf{w}_t$ and $\mathbf{e}_t$, are zero-mean normally distributed random variables with covariance matrices $\boldsymbol{\Gamma}$ and $\boldsymbol{\Sigma}$, respectively.

The initial latent state is assumed to be distributed as $\mathbf{y}_1\sim\mathcal{N}(\boldsymbol{\mu}_0,\mathbf{V}_0)$. Only the output of the system is observed, the state and all the noise variables are hidden. Given the observation sequence, the parameters $\{\mathbf{A},\mathbf{C},\boldsymbol{\Gamma},\boldsymbol{\Sigma},\boldsymbol{\mu}_0,\mathbf{V}_0\}$ can be learned by the expectation maximization (EM) method. The procedure iterates an E-step – Kalman smoothing recursion that fixes the current parameters and computes posterior probabilities over the hidden states given the observations, and an M-step that maximizes the expected log likelihood of the parameters using the posterior distribution computed in E-step. The comparison of features before and after smoothing by using the LDS approach is shown in Fig. 5. It can be seen that there is a general trend in feature before smoothing by using the LDS approach, but disordered in details. On the contrary, the details are smoothed after using the LDS approach, and the noise irrelevant to emotion is mostly removed.

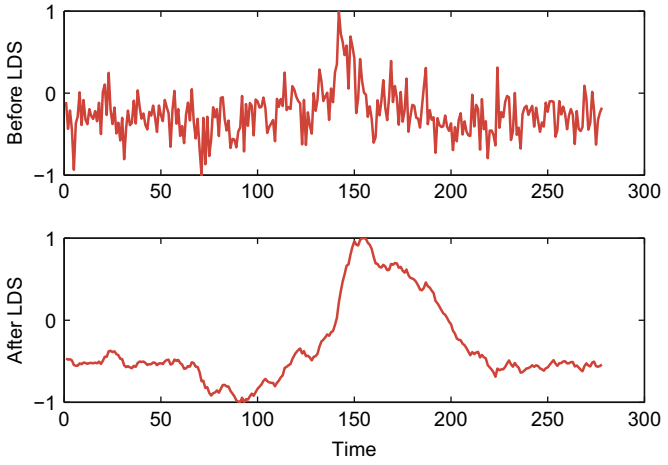

Fig. 5. Comparison of the power spectrum features of frequency domain before and after using the LDS method for feature smoothing. The features were obtained from channel P8 at alpha band in session 8 of subject 1.

4.4. Feature dimensionality reduction

Feature dimensionality reduction is an important step in EEG data analysis. It can not only improve learning efficiency, but also improve prediction performance. In this paper, feature dimensionality reduction was carried out with three well known dimensionality reduction methods, namely principal component analysis (PCA), linear discriminant analysis (LDA), and correlation-based feature selector (CFS).

4.4.1. Principal component analysis

Principal component analysis is a well-established method for feature extraction and dimensionality reduction. The main idea of principal component analysis is to represent data in a space that best expresses the variation in a sum-squared error sense. Given an m dimension EEG feature set $\mathbf{X}$, where $\mathbf{X}$ is an $m\times n$ matrix and n denotes the number of samples. First, the m dimensional mean vector $\boldsymbol{\mu}$ and $m\times m$ covariance matrix $\boldsymbol{\Sigma}$ are computed for the full feature set. Second, the eigenvectors and eigenvalues are computed, and sorted according to decreasing eigenvalue. Call these eigenvectors $\mathbf{e}_1$ with eigenvalue λ_1, $\mathbf{e}_2$ with eigenvalue λ_2, and so on. Subsequently, the largest k eigenvectors are chosen, and an $m\times k$ matrix $\mathbf{A}$ whose columns consist of the k eigenvectors is generated. Finally, the given data can be preprocessed as follows:

$$\mathbf{x}_{pca} = \mathbf{A}^T(\mathbf{x}-\boldsymbol{\mu}) \tag{15}$$

It can be shown that this representation minimizes a squared error criterion [61].

4.4.2. Linear discriminant analysis

Linear discriminant analysis is a traditional solution to the linear dimension reduction problem, which is based on the maximization of the between-class scatter over the within-class scatter. Give an EEG feature set $\{\mathbf{x}_i,y_i\}$, where $\mathbf{x}_i\in\mathbb{R}^m$ is the feature sample and $y_i\in\{-1,1\}$ is the class label. A direction $\alpha\in\mathbb{R}^d$ in the predictor space in which the classes are separated as much as possible is searched. This problem can be expressed as the

following criterion:

$$\max_{\alpha}\frac{\alpha^T\mathbf{B}\alpha}{\alpha^T\mathbf{W}\alpha} \tag{16}$$

where $\mathbf{B}$ is the between-class covariance matrix and $\mathbf{W}$ is the within-class covariance matrix. Give any direction $\alpha\in\mathbb{R}^m$, if the data is projected onto α, then the numerator of Eq. (16) is the marginal between-class variance and the denominator, the marginal within-class variance. The optimal solution of this problem is the first eigenvector of $\mathbf{W}^{-1}\mathbf{B}$. Given the first $(m-1)$ discriminant directions, the m-th direction can be obtained by

$$\arg\max_{\alpha}\frac{\alpha^T\mathbf{B}\alpha}{\alpha^T\mathbf{W}\alpha} \quad \text{subject to } \alpha^T\mathbf{W}\alpha_j \quad \forall j<m. \tag{17}$$

The optimal discriminant directions are the extracted features, which are the most important features for classification.

4.4.3. Correlation-based feature selector

Correlation-based feature selector is a kind of supervised dimensionality reduction method. Each feature gets a score presenting its correlation with emotion by this method. The most emotion-relevant features can be found by ranking these scores.

Let EEG feature set be denoted by $m\times n$ matrix $\mathbf{X}$, where m is the dimension of features and n is the number of samples, then $\mathbf{X}=\{\mathbf{x}_1,\mathbf{x}_2,\ldots,\mathbf{x}_n\}$. Let $\mathbf{r}_i^T$ denote the random variable corresponding to the i-th component of $\mathbf{x}$, $i=1,2,\ldots,m$, and $\mathbf{y}$ denote the label set of samples. The emotion-relevant score of each feature can be computed as follows:

$$R_{\mathbf{r}_i\mathbf{y}}=\frac{C_{\mathbf{r}_i\mathbf{y}}}{\sqrt{C_{\mathbf{r}_i}C_{\mathbf{y}}}}. \tag{18}$$

where C represents covariance and R denotes the correlation coefficient. The absolute value of correlation coefficient can be regarded as emotion-relevant score. Ranking these scores in a descending order, the top-ranked features are considered as the most emotion-relevant features.

4.5. Classification

To assess the association between EEG and emotional states, the classification into the predefined emotional classes was achieved by using support vector machine (SVM) classifiers [62]. Basically, SVM is to construct a separating hyperplane between two classes, the positive and negative examples, in such a way that the distance from each of the two classes to the hyperplane is maximized. Consider the problem of separating the set of training vectors belonging to two separate classes $\mathbf{G}=\{(\mathbf{x}_i,y_i),i=1,2,\ldots,n\}$, here $\mathbf{x}_i\in\mathbb{R}^m$ is the i-th input vector and $y_i\in\{-1,1\}$ is the binary target. The equation of the hyperplane separating two different classes is given by the following equation:

$$y(\mathbf{x})=\mathbf{w}^T\boldsymbol{\varphi}(\mathbf{x})+b=0 \tag{19}$$

where $\boldsymbol{\varphi}:\mathbb{R}^m\to\mathbb{R}^r$ is the feature map mapping the input space to a high feature space, in which the data points become linearly separable. All operations in learning and testing modes are done in SVM using the so-called kernel functions. The kernel is defined as $k(\mathbf{x}_i,\mathbf{x}_j)=\boldsymbol{\varphi}^T(\mathbf{x}_i)\cdot\varphi(\mathbf{x}_j)$.

The problem of learning SVM, formulated as the task of separating learning vector $\mathbf{x}_i$ into two classes of the destination values either $y_i=1$ or $y_i=-1$ with maximal separation margin, is reduced to the dual maximization problem of the function $Q(\alpha)$ defined as follows:

$$Q(\alpha)=\sum_{i=1}^{n}\alpha_i-\frac{1}{2}\sum_{i=1}^{n}\sum_{j=1}^{n}\alpha_i\alpha_j y_i y_j k(\mathbf{x}_i,\mathbf{x}_j) \tag{20}$$

with the constraints

$$\sum_{i=1}^{n}\alpha_i y_i=0 \quad 0\le\alpha_i\le C \tag{21}$$

where C is a user-defined constant. It is a regulation parameter and determines the balance between the complexity of the network, characterized by the weight vector $\mathbf{w}$ and the error of classification of data.

4.6. Trajectory of emotion changes

In the above analysis, we mainly focus on the emotion classification, but emotion usually changes step by step. Thus, we use manifold learning to find the trajectory of emotion changes.

In this paper, the Isomap method is chosen for its global characteristics. Isomap seeks to preserve the intrinsic geometry of the nonlinear data by utilizing the geodesic manifold distances between the data points [63]. The algorithm can be divided into three steps. (a) Construction of global neighborhood graph. For each point, find its k nearest neighbors using the predefined conditions. Construct a neighborhood graph by connecting each point to its k neighbors, with the distance of the points in the original spaces as the edge weights. (b) Computation of shortest paths. Estimate the shortest paths $d_{i,j}$ between each pair of points i, j as geodesic distance. The shortest paths were computed by Dijkstra method with the global neighborhood graph. (c) Construction of embedding. After calculation of the shortest paths, the data can be represented with a matrix $\mathbf{D}=\{d_{i,j}^2\}$, expressing the geodesic distance of each pair of points on the manifold. Applying classical multidimensional scaling (MDS) to this matrix constructs an embedding of the data that best preserves the manifold's estimated intrinsic geometry. Assume that

$$\mathbf{K}=-\tfrac{1}{2}(\mathbf{I}-\mathbf{e}\mathbf{e}^T)\mathbf{D}(\mathbf{I}-\mathbf{e}\mathbf{e}^T), \tag{22}$$

with $\mathbf{e}=1/n(1,1,\ldots,1)^T$. The largest k eigenvalues of $\mathbf{K}$ are $\lambda_1,\lambda_2,\ldots,\lambda_k$ and the respective eigenvectors are $\mathbf{u}_1,\mathbf{u}_2,\ldots,\mathbf{u}_k$. Assume $\mathbf{U}=(\mathbf{u}_1,\mathbf{u}_2,\ldots,\mathbf{u}_k)$, then the embedding result is

$$\mathbf{F}=diag(\sqrt{\lambda_1},\sqrt{\lambda_2},\ldots,\sqrt{\lambda_k})\mathbf{U}^T. \tag{23}$$

The selected features we got from feature dimensionality reduction were input to the Isomap model and output with one dimension. This one dimension curve is the trajectory of emotion changes.

5. Experimental results and discussions

In order to perform a more reliable classification process, we constructed a training set and a test set for each subject. The training set was formed by the former four sessions of EEG data for each emotional state. The test set was formed by the last two sessions of EEG data for each emotional state. The number of feature dimension equals the product of the number of features obtained for each trial of the EEG signal and the number of scalp electrodes.

5.1. Time windows

To find the most suitable time window length, we compared the classification performance using power spectrum across all EEG frequency bands with four different length time windows of 0.5 s, 1 s, 1.5 s, and 2 s. The linear SVM classifier was applied to these four kinds of features. The classification results are presented in Table 3. It can be seen that the average classification accuracy of 1 s EEG epoches is better than those of others. Hence, 1 s was chosen as the time window length in the remaining paper. In this

Table 3
Classification accuracies of power spectrum across all EEG frequency bands with different length time windows.

Subject	0.5 s (%)	1 s (%)	1.5 s (%)	2 s (%)
1	96.28	99.63	91.72	85.64
2	80.99	81.95	70.55	77.04
3	91.26	87.16	77.95	70.45
4	89.38	91.13	100	83.11
5	82.05	82.90	83.78	80.26
6	84.10	82.39	78.64	77.60
Average	87.34	**87.53**	83.77	79.07

Table 4
Classification accuracies of power spectrum across all frequency bands with or without LDS smoothing.

Subject	Feature smoothing	Delta	Theta	Alpha	Beta	Gamma	All
1	Without LDS	59.43	61.31	83.82	79.28	88.55	91.62
	With LDS	68.23	66.21	92.38	82.83	100	99.63
2	Without LDS	47.88	77.69	84.83	87.92	68.63	77.87
	With LDS	57.58	87.09	86.30	72.86	73.65	81.95
3	Without LDS	82.37	62.52	74.92	78.26	82.57	84.89
	With LDS	91.30	77.74	84.06	85.82	91.20	87.16
4	Without LDS	41.73	63.82	61.29	89.01	79.42	87.14
	With LDS	38.80	74.28	65.63	100	88.47	91.13
5	Without LDS	43.47	67.79	81.71	64.20	60.31	68.55
	With LDS	45.81	74.19	90.48	77.42	62.26	82.90
6	Without LDS	66.21	77.32	86.82	76.37	78.22	87.23
	With LDS	71.24	84.65	94.35	82.71	89.82	82.39
Average	Without LDS	56.85	68.40	78.89	79.17	76.28	82.88
	With LDS	62.16	77.36	85.53	83.61	84.23	**87.53**

Here, 'All' means the combination of five EEG power spectrum features.

case, the numbers of training data and test data are 1800 and 700, respectively.

5.2. Effect of feature smoothing

To validate the effect of feature smoothing, we compared the classification results of power spectrum across different EEG frequency bands with or without LDS smoothing. The linear SVM was chosen as classifier. Table 4 shows the classification performance obtained by SVM classifiers. It can be seen that almost all the classification accuracies are improved, which are significant improvement compared to the case when LDS smoothing is not employed. This result indicates that using the feature smoothing technique can effectively improve classification performance.

5.3. Choosing SVM kernels

One of our motivation is to search the best performance of classification of emotional states. In this study, the SVM classifier was used for classification. To find the best kernel of SVM, the performance of three different kinds of kernels, namely linear, polynomial and RBF, was compared in our experiments. The parameters of SVM were determined by 10-fold cross validation method. For linear SVM, we estimated the classification accuracy using different cost parameters C: $C \in \{2^{-4}, 2^{-3}, \ldots, 2^{9}, 2^{10}\}$. For polynomial SVM, we studied the validation accuracy using different combinations of the cost parameter C and polynomial degree of d: $C \in \{2^{-4}, 2^{-3}, \ldots, 2^{9}, 2^{10}\}$ and $d \in \{1, 2, \ldots, 14, 15\}$. For RBF SVM, we used the different combinations of the cost parameter C and kernel parameter γ: $C \in \{2^{-4}, 2^{-3}, \ldots, 2^{9}, 2^{10}\}$ and $\gamma \in \{2^{-10}, 2^{-9}, \ldots, 2^{3}, 2^{4}\}$. The code of SVMs was from LibSVM [64]. The experiments were performed on a computer with 8 GB RAM and 2.83 GHz CPU. Table 5 presents the classification performance of power spectrum across all frequency bands using SVM with linear, polynomial and RBF kernels.

Table 5
Classification accuracies of power spectrum across different frequency bands using SVMs with different kernels.

Subject	Kernel function	Delta	Theta	Alpha	Beta	Gamma	All
1	Linear	68.23	66.21	92.38	82.83	100	99.63
	Poly	66.30	73.65	78.51	68.60	97.70	99.36
	RBF	69.51	75.67	80.72	84.02	100	91.55
2	Linear	57.58	87.09	86.30	72.86	73.65	81.95
	Poly	63.37	77.34	70.22	92.09	86.17	84.59
	RBF	70.09	90.91	87.62	76.68	73.12	74.70
3	Linear	91.30	77.74	84.06	85.82	91.20	87.16
	Poly	86.44	83.13	97.21	92.13	89.75	75.47
	RBF	89.86	80.12	83.33	85.71	83.23	74.02
4	Linear	38.80	74.28	65.63	100	88.47	91.13
	Poly	52.55	68.96	21.06	73.84	82.71	76.05
	RBF	47.45	49.45	49.45	74.50	73.61	49.67
5	Linear	45.81	74.19	90.48	77.42	62.26	82.90
	Poly	68.06	78.06	87.10	67.26	74.03	68.39
	RBF	50.32	78.23	90.97	58.87	68.87	67.26
6	Linear	71.24	84.65	94.35	82.71	89.82	82.39
	Poly	70.76	72.54	76.09	86.11	92.41	88.69
	RBF	66.24	85.30	90.95	79.32	79.00	77.38
Average	Linear	62.16	77.36	85.53	83.61	84.23	**87.53**
	Poly	67.91	75.61	71.70	80.01	87.13	82.09
	RBF	65.58	76.61	80.51	76.52	79.64	72.43

Here, 'All' means the combination of five EEG power spectrum features.

Table 6
Classification accuracies of power spectrum of differential asymmetry features.

Subject	Delta	Theta	Alpha	Beta	Gamma	All
1	71.62	57.76	67.13	75.85	87.42	86.41
2	52.04	47.83	65.35	96.44	84.85	93.67
3	65.42	74.22	53.44	63.73	66.21	66.62
4	41.02	40.80	72.06	100.00	99.33	100.00
5	54.19	48.06	64.68	34.52	66.77	63.71
6	57.51	71.41	79.16	87.88	93.21	93.86
Average	50.30	53.34	63.64	74.74	81.30	**82.38**

Here, 'All' means the combination of five EEG frequency domain features.

From Table 5, several important observations can be drawn. Firstly, it can be observed that the classification performance of power spectrum across all frequency bands is better than those based on individual frequency bands under the same conditions. Secondly, it is found that the classification performance of alpha, beta and gamma bands is obviously better than those of delta and theta bands. This result partly reflects that high frequency bands play a more important role in emotion activities than low frequency bands [65,66]. Finally, the average classification performance of SVM with linear kernel outperforms SVM with polynomial kernel and RBF kernel. The average classification accuracy of power spectrum across all frequency bands using SVM with linear kernel is 87.53%. This definitely proves the robustness of the linear SVM over the polynomial and RBF SVM for these data sets, so that SVM with linear kernel was chosen as the basic classifier in the remaining paper.

5.4. Comparison of power spectrum with other features

To find the best emotion-specific features of EEG, other kinds of features were also applied in this study. Table 6 shows the classification performance of the power spectrum of differential asymmetry features. It can be found that the classification performance of the combination of all power spectrum of differential asymmetry features is better than those based on individual frequency band features under the same conditions. The average accuracy with the combination of all power spectrum of differential asymmetry features is 82.38% using SVM. Table 7 shows the classification performance of the wavelet features. As we can see, the average classification performance of wavelet entropy across all frequency bands is better than other wavelet features. A maximum classification accuracy of 78.41% is obtained using the wavelet entropy across all frequency bands. Table 8 shows the classification performance using nonlinear dynamical features. From Table 8, it can be found that the hurst exponent feature gives a maximum average classification accuracy of 71.38% over other nonlinear dynamical features.

Table 7
Classification accuracies of wavelet features across different frequency bands using linear SVM.

Subject	A5	D5	D4	D3	D2	All	Wavelet entropy
1	64.46	49.12	52.61	72.36	71.90	71.81	72.64
2	33.86	87.61	87.87	70.48	63.21	67.85	64.30
3	83.54	32.61	76.71	81.06	66.87	82.37	80.12
4	41.02	57.43	50.55	80.48	83.81	76.50	97.11
5	57.10	60.32	56.61	65.65	49.03	65.00	65.81
6	33.60	95.15	77.22	91.60	88.85	99.35	90.47
Average	52.26	63.70	66.93	76.94	70.61	77.14	**78.41**

Here, 'All' means the combination of wavelet coefficient energy across all EEG frequency bands.

Table 8
Classification accuracies of nonlinear dynamical feature using linear SVM.

Subject	Approximate entropy	Hurst exponent	Fractal dimension
1	51.33	68.68	85.22
2	69.96	88.27	66.93
3	77.32	66.77	55.48
4	50.55	38.80	74.28
5	70.81	68.06	54.83
6	70.76	97.74	87.07
Average	65.12	**71.38**	70.63

From the above analysis, though the classification performance exists some individual differences among subjects, the average classification performance confirms that power spectrum across all frequency bands is the most robust feature among all of the three kinds of features discussed above.

5.5. Comparison of feature dimensionality reduction methods

One of the purposes of our study is to find the relationship between EEG data and emotional states. Moreover, we want to find the general subject-independent features related to emotion. Thus, feature dimensionality reduction was important in our study. Because the best performance was obtained using the power spectrum across all frequencies, three kinds of dimensionality reduction methods, namely PCA, LDA and CFS, were applied to this type of feature for further data analysis.

Fig. 6 illustrates the classification accuracy of using the PCA approach. The horizontal axis denotes the number of principle components used for classification, and the vertical axis denotes the classification accuracy. It is shown that when the feature dimension reaches a certain number, the classification accuracy becomes almost stable. Obviously this number is much smaller than the dimension of the original features.

The classification performance of the LDA method is shown in Fig. 7. For most subjects, when the feature dimension reaches a certain number, the classification accuracy becomes almost stable. This number is much smaller than the dimension of the original features. However, there exist greater individual differences in performance among the six subjects.

The classification performance of the CFS approach is shown in Fig. 8. When the dimension of features reaches about 100, the

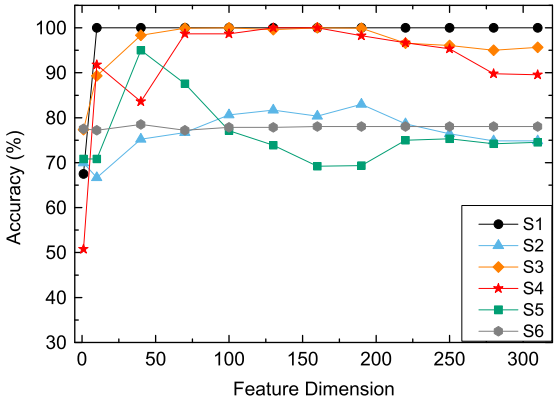

Fig. 7. The process of LDA.

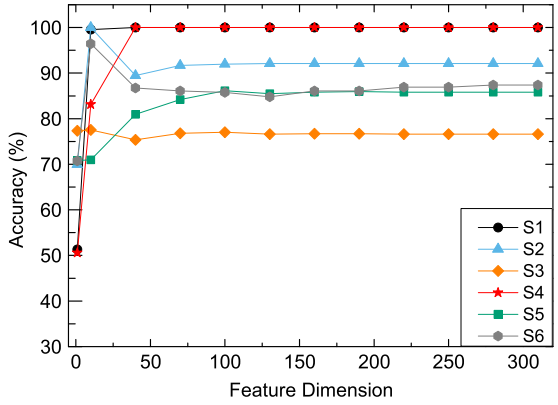

Fig. 6. The process of PCA.

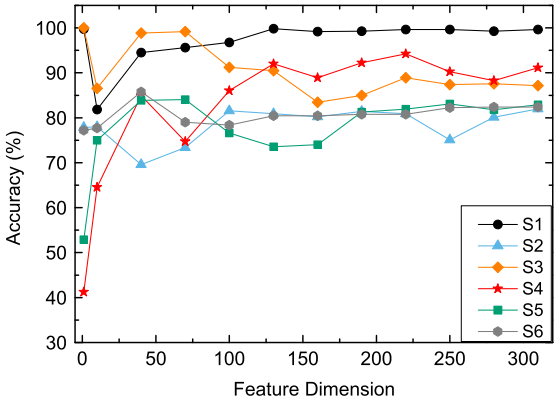

Fig. 8. The process of CFS.

accuracy of classification becomes almost stable, and the average accuracy is about 85.25%. Obviously this number is much smaller than the dimension of the original features. Considering the characteristics of CFS, we could confirm that not all the brain areas and EEG frequency bands were related with emotion. This observation provides the possibility to find subject-independent features among subjects.

To compare these three different methods for feature dimensionality reduction, the average classification accuracies of these methods are computed and shown in Fig. 9. It can be seen that the best average accuracy of 91.77% is obtained by the LDA method when the number of feature dimensions is reduced to 30, whereas the average performance of the PCA method is a bit better and more stable. The merit of PCA is that the extracted features have the minimum correlation along the principal axes, but PCA cannot be used to find the emotion-specific features. In contrast, the features selected by CFS were directly computed from features. Therefore, the emotion-related brain areas and frequency bands could be found by CFS.

5.6. Subject-independent features

In order to confirm the existence of subject-independent features, we tried to find the relationship between feature dimension and the electrode amount. First we calculated the average correlation coefficients of all subjects and ranked the coefficients in descending order. Then we reduced progressively the number of features with ascending coefficients, and computed the number of electrodes needed. The result is shown in Fig. 10. When feature dimension reaches a certain number, the number of electrode decreases quickly with the reduction of feature dimension. Thus, we could assume that the subject-independent features related with emotion centralized distributed on head regions.

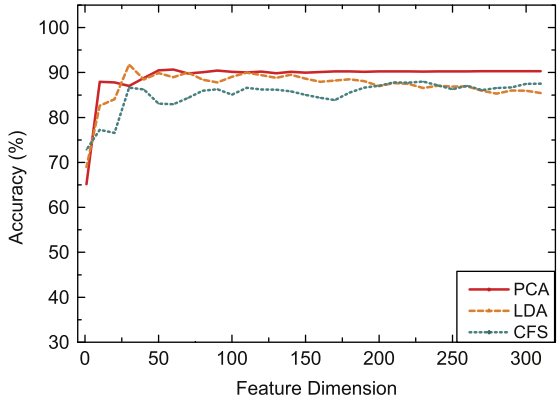

Fig. 9. The average results of three different dimension reduction methods for power spectrum across all EEG frequency bands.

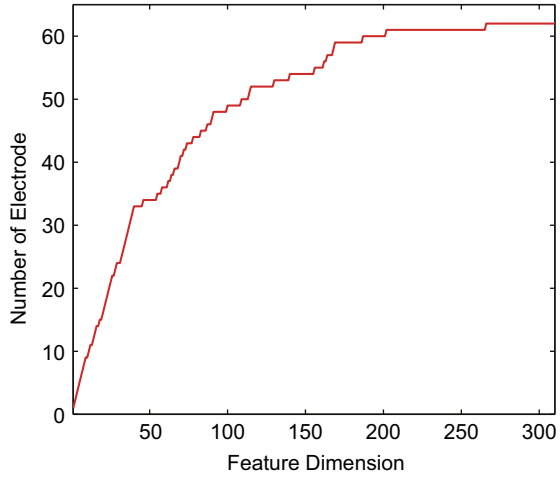

Fig. 10. The relationship between feature dimension and the number of electrodes.

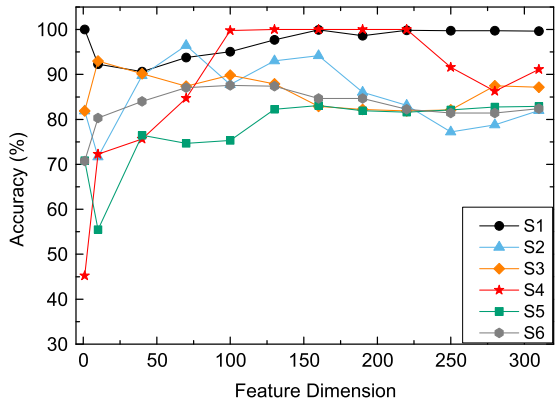

Fig. 11. The classification performance of subject-independent features.

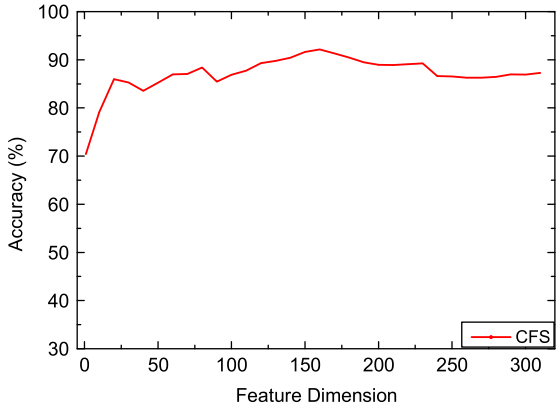

Fig. 12. The average classification performance of subject-independent features.

Here the CFS method was used to find these subject-independent features. The features were incorporated progressively with average correlation coefficients in descending order. The classification performance of subject-independent features is shown in Fig. 11. Compared with Fig. 8, the classification performance is degraded. As shown in Fig. 12, the average accuracy with the top 100 subject-independent features is 84.90%. The classification accuracies of most subjects become stable after the dimension reaches about 40 and the average accuracy is 83.55%. The distribution of the top 50 subject-independent features is shown in Fig. 13. None of the top 50 features are in the delta band and few were in the theta band. This suggests that delta and theta bands have little relationship with emotion. The selected subject-independent features were mainly in the right occipital lobe and parietal lobe for the alpha band, the parietal lobe and temporal lobe for beta band, and the left frontal lobe and right temporal lobe for gamma band. This finding is nearly consistent with the studies of other researchers [67–70].

5.7. Trajectory of emotion changes

In order to find the trajectory of emotion changes during the experiment, we put the selected 50 subject-independent features into the manifold model and reduced the features into one dimension using the Isomap method. The trajectory of emotion changes is shown in Fig. 14. The dashed (red) line represents the

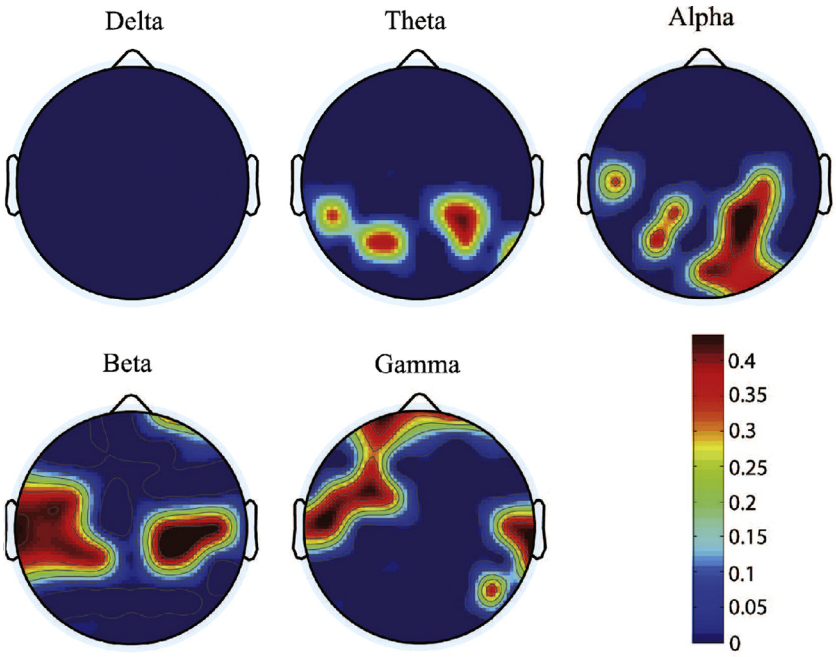

Fig. 13. Distribution of the top 50 subject-independent features.

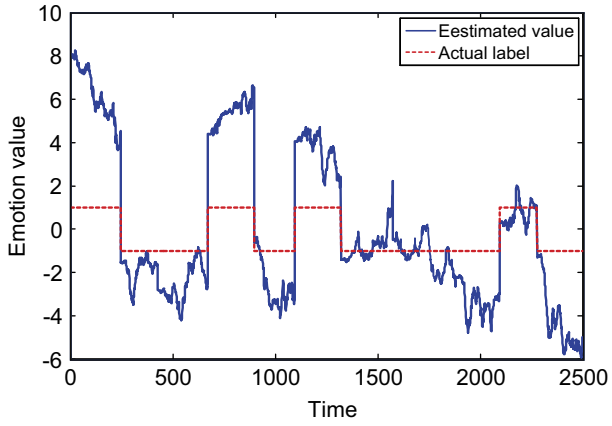

Fig. 14. The trajectory of emotion changes of subject 6 during the experiment. (For interpretation of the references to color in this figure caption, the reader is referred to the web version of this paper.)

emotional states labels, where positive emotion is labeled as $+1$ and negative emotion is labeled as -1. The solid (blue) line indicates the values of Isomap estimation. It can be seen that the changes of the trajectory obtained by Isomap are almost consistent with the change of emotional states.

In summary, power spectrum across all frequency bands extracted from EEG signals performs well on distinguishing positive and negative emotional states. The emotion-specific feature is mainly related to high frequency band rather than low frequency band. The subject-independent feature is mainly on right occipital lobe and parietal lobe in alpha band, the parietal lobe and temporal lobe in beta band, left frontal lobe and right temporal lobe in gamma band.

6. Conclusions

In this paper, we have investigated the characteristics of EEG features for emotion classification and technique for tracking the trajectory of emotion changes. A series of experiments of using movie clips are designed to arouse emotion of subjects and an EEG data set of six subjects is collected. Three kinds of features, namely power spectrum, wavelet and nonlinear dynamical analysis, are extracted to assess the association between the EEG data and emotional states. All of these features are smoothed by the LDS method to remove the noise unrelated with emotion. The results of emotion classification by SVM classifiers show that the LDS method can improve classification accuracy significantly. Experimental results demonstrate that power spectrum across all frequency bands is the most robust feature among all three kinds of features discussed above, and high frequency bands play a more important role in emotion activities than low frequency bands.

Furthermore, three dimensionality reduction methods, namely PCA, LDA and CFS, are adopted and further compared on the feature set. The best average classification accuracy of 91.77% is obtained by using the LDA method when the number of feature dimensions is reduced to 30. The top 50 subject-independent features most relevant to emotion are selected by the CFS method. Through these subject-independent features, we found that the emotion associated EEG is mainly produced in the right occipital lobe and parietal lobe for the alpha band, the parietal lobe and temporal lobe for beta band, and the left frontal lobe and right temporal lobe for gamma band. The trajectory of emotion changes is drawn by a manifold learning model. This provides a promising way of implementing visualization of subject's emotional state in real time.

The future development of this research will be focused on increasing the number of subjects and the number of experiments for each of the subjects, and extracting subject-independent features that can eliminate the inter-subjective variability. We also would like to explore multi-modal analysis for emotion classification.

Acknowledgments

This work was supported partially by the National Basic Research Program of China (Grant no. 2013CB329401 and Grant no. 2009CB320901), the National Natural Science Foundation of

China (Grant no. 61272248), and the Science and Technology Commission of Shanghai Municipality (Grant no. 13511500200).

References

[1] R. Picard, Affective Computing, MIT press, 2000.
[2] V. Petrushin, Emotion in speech: recognition and application to call centers, in: Proceedings of the Artificial Networks in Engineering Conference, 1999, pp. 7–10.
[3] M. Black, Y. Yacoob, Recognizing facial expressions in image sequences using local parameterized models of image motion, Int. J. Comput. Vis. 25 (1997) 23–48.
[4] K. Anderson, P. McOwan, A real-time automated system for the recognition of human facial expressions, IEEE Trans. Syst. Man Cybern. B Cybern. 36 (2006) 96–105.
[5] J. Wagner, J. Kim, From physiological signals to emotions: Implementing and comparing selected methods for feature extraction and classification, in: Proceedings of IEEE International Conference on Multimedia and Expo, 2005, pp. 940–943.
[6] K. Kim, S. Bang, S. Kim, Emotion recognition system using short-term monitoring of physiological signals, Med. Biol. Eng. Comput. 42 (2004) 419–427.
[7] J. Brosschot, J. Thayer, Heart rate response is longer after negative emotions than after positive emotions, Int. J. Psychophysiol. 50 (2003) 181–187.
[8] J. Coan, J. Allen, Frontal EEG asymmetry as a moderator and mediator of emotion, Biol. Psychol. 67 (2004) 7–50.
[9] P. Petrantonakis, L. Hadjileontiadis, A novel emotion elicitation index using frontal brain asymmetry for enhanced EEG-based emotion recognition, IEEE Trans. Inf. Technol. Biomed. 15 (2011) 737–746.
[10] X. Li, B. Hu, T. Zhu, J. Yan, F. Zheng, Towards affective learning with an EEG feedback approach, in: Proceedings of the 1st ACM International Workshop on Multimedia Technologies for Distance Learning, 2009, pp. 33–38.
[11] R. Davidson, N. Fox, Asymmetrical brain activity discriminates between positive and negative affective stimuli in human infants, Science 218 (1982) 1235.
[12] E. Harmon-Jones, J.J. Allen, et al., Anger and frontal brain activity: EEG asymmetry consistent with approach motivation despite negative affective valence, J. Personal. Soc. Psychol. 74 (1998) 1310–1316.
[13] E. Harmon-Jones, J.J. Allen, et al., Behavioral activation sensitivity and resting frontal EEG asymmetry: covariation of putative indicators related to risk for mood disorders, J. Abnorm. Psychol. 106 (1997) 159–163.
[14] A.J. Tomarken, R.J. Davidson, R.E. Wheeler, L. Kinney, Psychometric properties of resting anterior EEG asymmetry: temporal stability and internal consistency, Psychophysiology 29 (1992) 576–592.
[15] H.T. Schupp, B.N. Cuthbert, M.M. Bradley, J.T. Cacioppo, T. Ito, P.J. Lang, Affective picture processing: the late positive potential is modulated by motivational relevance, Psychophysiology 37 (2000) 257–261.
[16] D. Pizzagalli, M. Regard, D. Lehmann, Rapid emotional face processing in the human right and left brain hemispheres: an ERP study, Neuroreport 10 (1999) 2691–2698.
[17] M. Eimer, A. Holmes, An ERP study on the time course of emotional face processing, Neuroreport 13 (2002) 427–431.
[18] B. Weiner, Attribution, emotion, and action, Handbook of Motivation and Cognition: Foundations of Social Behavior 1 (1986) 281–312.
[19] T. Kemper, A Social Interactional Theory of Emotions, Wiley, New York, 1978.
[20] R. Davidson, G. Schwartz, C. Saron, J. Bennett, D. Goleman, Frontal versus parietal EEG asymmetry during positive and negative affect, Psychophysiology 16 (1979) 202–203.
[21] P. Ekman, R. Davidson, The Nature of Emotion: Fundamental Questions, Oxford University Press, 1994.
[22] G.L. Ahern, G.E. Schwartz, Differential lateralization for positive and negative emotion in the human brain: EEG spectral analysis, Neuropsychologia 23 (1985) 745–755.
[23] P. Lang, A. Ohman, D. Vaitl, The International Affective Picture System (Photographic Slides), Center for Research in Psychophysiology, University of Florida, Gainesville, FL, 1988.
[24] C. Alm, D. Roth, R. Sproat, Emotions from text: machine learning for text-based emotion prediction, in: Proceedings of the Conference on Human Language Technology and Empirical Methods in Natural Language Processing, 2005, pp. 579–586.
[25] K. Scherer, Which emotions can be induced by music? what are the underlying mechanisms? and how can we measure them? J. New Music Res. 33 (2004) 239–251.
[26] W. Hubert, R. de Jong-Meyer, Autonomic, neuroendocrine, and subjective responses to emotion-inducing film stimuli, Int. J. Psychophysiol. 11 (1991) 131–140.
[27] R. Lazarus, A Laboratory Study of Psychological Stress Produced by a Motion Picture Film, American Psychological Association, 1962.
[28] W. Hubert, R. de Jong-Meyer, Psychophysiological response patterns to positive and negative film stimuli, Biol. Psychol. 31 (1990) 73–93.
[29] P. Philippot, Inducing and assessing differentiated emotion-feeling states in the laboratory, Cogn. Emot. 7 (1993) 171–193.
[30] J. Hewig, D. Hagemann, J. Seifert, M. Gollwitzer, E. Naumann, D. Bartussek, A revised film set for the induction of basic emotions, Cogn. Emot. 19 (2005) 1095.
[31] J.J. Gross, R.W. Levenson, Emotion elicitation using films, Cogn. Emot. 9 (1995) 87–108.
[32] J. Estepp, S. Klosterman, J. Christensen, An assessment of non-stationarity in physiological cognitive state assessment using artificial neural networks, in: Proceedings of International Conference of the IEEE Engineering in Medicine and Biology Society, 2011, pp. 6552–6555.
[33] D. Nie, X. Wang, L. Shi, B. Lu, EEG-based emotion recognition during watching movies, in: Proceedings of International IEEE/EMBS Conference on Neural Engineering, 2011, pp. 667–670.
[34] D. Nie, Emotion recognition based on EEG (Master's thesis), Shanghai Jiao Tong University, Shanghai, 2012 (in Chinese).
[35] R. Davidson, Anterior electrophysiological asymmetries, emotion, and depression: conceptual and methodological conundrums, Psychophysiology 35 (1998) 607–614.
[36] J. Henriques, R. Davidson, Left frontal hypoactivation in depression, J. Abnorm. Psychol. 100 (1991) 535.
[37] T. Baumgartner, M. Esslen, L. Jancke, From emotion perception to emotion experience: emotions evoked by pictures and classical music, Int. J. Psychophysiol. 60 (2006) 34–43.
[38] R.D. Vanderploeg, W.S. Brown, J.T. Marsh, Judgements of emotion in words and faces: ERP correlates, Int. J. Psychophysiol. 5 (1987) 193–205.
[39] W. Sato, T. Kochiyama, S. Yoshikawa, M. Matsumura, Emotional expression boosts early visual processing of the face: ERP recording and its decomposition by independent component analysis, Neuroreport 12 (2001) 709–714.
[40] L. Carretie, F. Mercado, M. Tapia, J.A. Hinojosa, Emotion, attention and the" negativity bias", studied through event-related potentials, Int. J. Psychophysiol. 41 (2001) 75–85.
[41] G. Chanel, J. Kronegg, D. Grandjean, T. Pun, Emotion assessment: arousal evaluation using EEGs and peripheral physiological signals, in: Proceedings of Multimedia Content Representation, Classification and Security, 2006, pp. 530–537.
[42] M. Li, B. Lu, Emotion classification based on gamma-band EEG, in: Proceedings of International Conference of the IEEE Engineering in Medicine and Biology Society, 2009, pp. 1223–1226.
[43] Q. Zhang, M. Lee, Analysis of positive and negative emotions in natural scene using brain activity and gist, Neurocomputing 72 (2009) 1302–1306.
[44] M. Murugappan, N. Ramachandran, Y. Sazali, Classification of human emotion from EEG using discrete wavelet transform, J. Biomed. Sci. Eng. 3 (2010) 390–396.
[45] P. Petrantonakis, L. Hadjileontiadis, Emotion recognition from EEG using higher order crossings, IEEE Trans. Inf. Technol. Biomed. 14 (2010) 186–197.
[46] M. Bradley, P. Lang, Measuring emotion: the self-assessment manikin and the semantic differential, J. Behav. Ther. Exp. Psychiatry 25 (1994) 49–59.
[47] D. Sammler, M. Grigutsch, T. Fritz, S. Koelsch, Music and emotion: electrophysiological correlates of the processing of pleasant and unpleasant music, Psychophysiology 44 (2007) 293–304.
[48] Y.-P. Lin, C.-H. Wang, T.-P. Jung, T.-L. Wu, S.-K. Jeng, J.-R. Duann, J.-H. Chen, EEG-based emotion recognition in music listening, IEEE Trans. Biomed. Eng. 57 (2010) 1798–1806.
[49] M. Murugappan, M. Rizon, R. Nagarajan, S. Yaacob, I. Zunaidi, D. Hazry, EEG feature extraction for classifying emotions using FCM and FKM, Int. J. Comput. Commun. 1 (2007) 21–25.
[50] A. Subasi, EEG signal classification using wavelet feature extraction and a mixture of expert model, Expert Syst. Appl. 32 (2007) 1084–1093.
[51] L. Aftanas, N. Lotova, V. Koshkarov, V. Pokrovskaja, S. Popov, V. Makhnev, Non-linear analysis of emotion EEG: calculation of Kolmogorov entropy and the principal Lyapunov exponent, Neurosci. Lett. 226 (1997) 13–16.
[52] S. Pincus, Approximate entropy (apen) as a complexity measure, Chaos Interdiscip. J. Nonlinear Sci. 5 (1995) 110–117.
[53] S.A. Hosseini, M.B. Naghibi-Sistani, Emotion recognition method using entropy analysis of EEG signals, Int. J. Image Graph. Signal Process. 3 (2011) 30.
[54] H. Hurst, Long-term storage capacity of reservoirs, American Society of Civil Engineering 76 (1950).
[55] N. Kannathal, U. Acharya, C. Lim, P. Sadasivan, Characterization of eegła comparative study, Comput. Methods Progr. Biomed. 80 (2005) 17–23.
[56] R. Khosrowabadi, A. Wahab bin Abdul Rahman, Classification of EEG correlates on emotion using features from Gaussian mixtures of EEG spectrogram, in: Proceedings of International Conference on Information and Communication Technology for the Muslim World, 2010, pp. 102–107.
[57] B.B. Mandelbrot, The Fractal Geometry of Nature, Times Books, 1983.
[58] A. Katz, A. Thompson, Fractal sandstone pores: implications for conductivity and pore formation, Phys. Rev. Lett. 54 (1985) 1325–1328.
[59] R. Acharya U, O. Faust, N. Kannathal, T. Chua, S. Laxminarayan, Non-linear analysis of EEG signals at various sleep stages, Comput. Methods Progr. Biomed. 80 (2005) 37–45.
[60] L. Shi, B. Lu, Off-line and on-line vigilance estimation based on linear dynamical system and manifold learning, in: Proceedings of International Conference of the IEEE Engineering in Medicine and Biology Society, 2010, pp. 6587–6590.
[61] I. Jolliffe, MyiLibrary, Principal Component Analysis, vol. 2, Wiley Online Library, 2002.
[62] V. Vapnik, Statistical Learning Theory, Wiley-Interscience, 1998.
[63] M. Balasubramanian, E. Schwartz, The isomap algorithm and topological stability, Science 295 (2002) 7.
[64] C. Chang, C. Lin, Libsvm: A Library for Support Vector Machines, Software Available at ⟨http://www.csie.ntu.edu.tw/~cjlin/libsvm⟩, 2001.

[65] W. Klimesch, EEG alpha and theta oscillations reflect cognitive and memory performance: a review and analysis, Brain Res. Rev. 29 (1999) 169–195.
[66] D. Oathes, W. Ray, A. Yamasaki, T. Borkovec, L. Castonguay, M. Newman, J. Nitschke, Worry, generalized anxiety disorder, and emotion: Evidence from the EEG gamma band, Biol. Psychol. 79 (2008) 165–170.
[67] W.J. Ray, H.W. Cole, EEG alpha activity reflects attentional demands, and beta activity reflects emotional and cognitive processes, Science 228 (1985) 750–752.
[68] R.J. Davidson, C.E. Schaffer, C. Saron, Effects of lateralized presentations of faces on self-reports of emotion and EEG asymmetry in depressed and non-depressed subjects, Psychophysiology 22 (1985) 353–364.
[69] B. Guntekin, E. Basar, Emotional face expressions are differentiated with brain oscillations, Int. J. Psychophysiol. 64 (2007) 91–100.
[70] D.J. Schutter, P. Putman, E. Hermans, J. van Honk, Parietal electroencephalogram beta asymmetry and selective attention to angry facial expressions in healthy human subjects, Neurosci. Lett. 314 (2001) 13–16.

Xiaowei Wang received his B.S. degree and the M.S. degree in computer science from Qingdao University, Qingdao, China, in 2002 and 2005, respectively. He is currently a Ph.D. candidate in the Brain-like Computing and Machine Intelligence Group, Shanghai Jiao Tong University. His research interests included biomedical engineering, biomechanical signal processing, machine learning and the development of brain–computer interface (BCI).

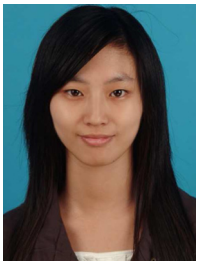

Dan Nie received the B.S. degree in computer science and engineering from Dalian University of Technology in 2009. She is currently a M.S. candidate in the Brain-like Computing and Machine Intelligence Group, Shanghai Jiao Tong University. Her research interests included statistical learning, signal processing and machine learning.

Bao-Liang Lu is received his B.S. degree from Qingdao University of Science and Technology, China, in 1982, the M.S. degree from Northwestern Polytechnical University, China, in 1989, and the Ph.D. degree from Kyoto University, Japan, in 1994. From 1982 to 1986, he was with the Qingdao University of Science and Technology. From April 1994 to March 1999, he was a Frontier Researcher at the Bio-Mimetic Control Research Center, the Institute of Physical and Chemical Research (RIKEN), Japan. From April 1999 to August 2002, he was a Research Scientist at the RIKEN Brain Science Institute. Since August 2002, he has been a full Professor at the Department of Computer Science and Engineering, Shanghai Jiao Tong University, China. His research interests include brain-like computing, neural networks, machine learning, pattern recognition, and brain–computer interface. He was the past President of the Asia Pacific Neural Network Assembly (APNNA) and the general Chair of ICONIP2011. He serves on the editorial board of Neural Networks Journal (Elsevier). He is a senior member of the IEEE.